論文の内容の要旨

論文題目：

Synthesis, Separation and Chirality-Specific Spectroscopy of Single-Walled Carbon Nanotubes

（単層カーボンナノチューブの合成・分離・カイラリティー依存分光）

趙　沛

1. Introduction

The single-walled carbon nanotube (SWNT), which is usually thought of as a sheet of graphene rolled into nanometer-sized cylinder, has been the subject of intense research since it was first discovered in 1993.[1] SWNTs have attracted enormous scientific attention on account of their extraordinary electrical, optical and mechanical properties resulting from their quasi-one-dimensional structure.[2] In this study, the synthesis, separation and chirality-specific spectroscopy of SWNTs was investigated. Using a post-growth application of the density gradient ultracentrifugation (DGU)[3,4] method, SWNTs dispersed by surfactants could be separated by chirality or electronic type, and were further characterized by optical spectroscopy. The synthesis of isotope-enriched suspended SWNTs was also achieved using no-flow alcohol catalytic chemical vapor deposition (ACCVD).[5] Corresponding Raman spectra[6] show a shortened lifetime for Γ-point optical phonons, which possibly results from an elastic scattering of those phonons.

2. Selective enrichment of SWNTs using DGU

Problems associated with single-chirality controlled synthesis of SWNTs still constitute one of the main obstacles to using this material in further applications. In this sense, post-growth treatment by physical or chemical techniques is expected to have an important role to play. There are a number of methods for separating SWNTs,[3,4,7-11] among which DGU[3,4], a surfactant-based technique, has proven to be effective in yielding high-quality SWNTs without intensive or complicated chemical or physical treatments. Since SWNTs themselves are hydrophobic, DGU separation is achieved by structure-dependent wrapping of ionic surfactants, which at the same time changes the buoyant densities of the SWNTs and facilitates their separation in a density-gradient medium.

Using the DGU technique, I present a protocol to controllably obtain a polychromatic “rainbow” dispersion containing seven different colored layers, as shown in Figure 1(a). This was achieved using a co-surfactant system containing sodium deoxycholate (DOC) and sodium dodecyl sulfate (SDS). Absorbance spectra show that the chiralities in the pristine sample are efficiently redistributed during DGU, and this redistribution has a strong dependence on the structure of the isolated species. The topmost violet layer contains primarily (*6*,*5*) SWNTs, which have the smallest diameter of those detected in the sample. The dominant species in each successive layer has an increasingly larger diameter, showing the redistribution is diameter-selective and separation is driven by difference in buoyant density.

Based on these observations I propose the following sorting mechanism. The strong interaction between the hydrophobic part of DOC and the nanotube sidewall[12] causes DOC to wrap around the nanotube with a preferred orientation. SDS fills the space between DOC molecules, enhancing the buoyancy. Most importantly, the

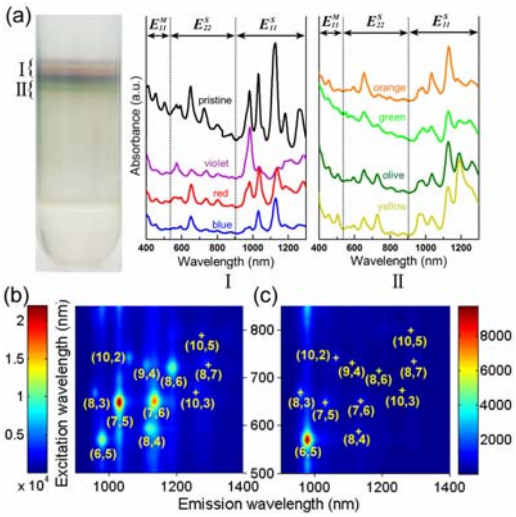

Figure 1. (a) Left: Photograph showing a multilayered separation “rainbow” of ACCVD SWNTs by density gradient ultracentrifugation. Right: Optical absorbance spectra of each colored fraction. (b,c) Normalized photoluminescence excitation (PLE) maps of the initial dispersion (b) and the topmost violet layer (c).

space between DOC molecules depends on the SWNT diameter, leading to a diameter-dependent enhancement in the density difference among SWNTs. This causes the expansion of the entire rainbow region after DGU.

This method not only illustrates the potential for complete isolation of a single (*n*,*m*) species, but also provides a simple way to better understand surfactant-nanotube interactions. Further understanding and refinement of this process is expected to lead to higher purity extraction of single-chirality SWNTs.

3. Tunable separation of SWNTs using dual-surfactant DGU method

I continue the discussion on dual-surfactant DGU of SWNTs by systematically investigating how those DOC and SDS influence the separation. A continuous enhancement of DGU separation of SWNTs is shown in Figure 2. All of these trials resulted in diameter-dependent separation, but increasing the concentration of SDS in the dispersion increasingly broadened the final separated region. In addition to this broadening, the position of each layer also shifted downward with increasing SDS concentration, indicating an overall increase in the density of the surfactant–SWNT micelles. Note that the lower layers shift more than the upper layers, and the highest concentrations of SDS (column 7) increased the density of the surfactant–SWNT micelles to such an extent that some of the larger diameter nanotubes (in the green and yellow layers) sank down to the bottom of the density gradient column. A proposed mechanism for this broadening is that continuous SDS loading into the space between DOC packed on the SWNT surfaces keeps increasing the density and density difference between nanotubes, which leads to a broadened separation region in the DGU column.

This finding provides a clearer understanding of the surfactant–SWNT interactions that govern the outcomes of DGU,

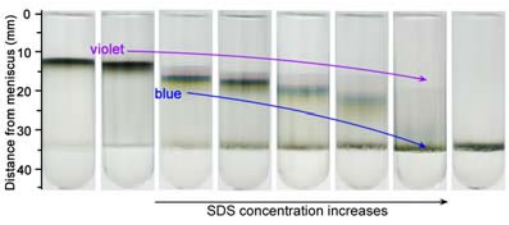

Figure 2. Co-surfactant DGU experimental results for the realization and expansion of the separated region using DOC and SDS.

and is helpful in designing DGU recipes such that desired results can be obtained with greater success.

4. Isotope-based investigation of SWNT-surfactant micelles

Different surfactants lead to different SWNT wrapping morphologies and form micelles of different sizes and buoyant densities. Various methods have been developed to obtain information about these SWNT-surfactant micelles, however, most of them are based on theoretical calculation or numerical simulation.[13-16] Experimentally, only a few approaches have been reported.[12,17,18] Considering that surfactants provide one of the most efficient non-covalent means of individually stabilizing SWNTs in aqueous dispersion, it is of great significance to develop more experimental approaches to improve the understanding of the micelles formed by surfactants and encapsulated SWNTs.

Here I present a novel approach to investigate the hydrodynamic information of surfactant- stabilized SWNT micelles in aqueous dispersion by analyzing the buoyant densities of isotopic SWNTs-surfactant micelles using the DGU method. SWNTs composed of ^{12}C or ^{13}C atoms were dispersed using three main types of surfactants: sodium cholate (SC), SDS and DOC. Analysis of the layer and density information after DGU experiments can provide information about the micelle volume by showing to what degree the surrounding layer can eliminate the density difference

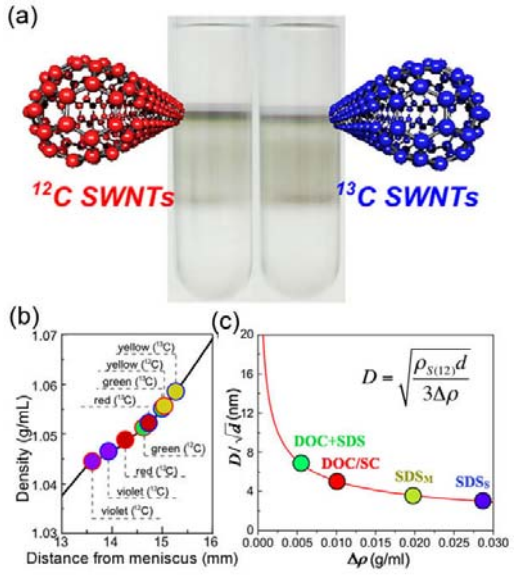

Figure 3. (a) DGU results from SC-dispersed ^{12}C and ^{13}C SWNTs. (b) The density gradient profile of each layer in SC-DGU experiments. (c) Corresponding layer thickness of different SWNT-surfactant micelles.

between bare ^{12}C and ^{13}C SWNTs, which is about 9% of the weight of a ^{12}C SWNT.

The buoyant density ρ of an SWNT-surfactant micelle can be expressed as

$$\rho = \frac{\rho_{S(12)}\pi d + \rho_{sur}\pi(\frac{D^2}{4} - \frac{d^2}{4}) + \rho_{in}(\frac{d^2}{4})}{\pi(\frac{D^2}{4})}$$

where $\rho_{S(12)}$ is the density of a ^{12}C graphene sheet, ρ_{sur} is the density of surrounding layer by surfactant and hydrated water, ρ_{in} is the density inside an SWNT, *D* is the diameter of the micelle and *d* is the diameter of the SWNT. Therefore, the diameter *D* of an SWNT-surfactant micelle can be calculated using the buoyant density difference between ^{12}C and ^{13}C SWNT micelles (Δρ):

$$D = \sqrt{\frac{\rho_{S(12)}d}{3\Delta\rho}}$$

Separation results using SC for ^{12}C and ^{13}C SWNTs are shown in Figure 3(a). The corresponding layer densities vs. density gradient profile plotted in Figure 3(b) show that the density differences between ^{12}C and ^{13}C are very small, approximately 0.005 g/mL, after wrapping by SC. Similar analysis on SDS, DOC and DOC+SDS system shows that SWNT micelles formed by bile salts

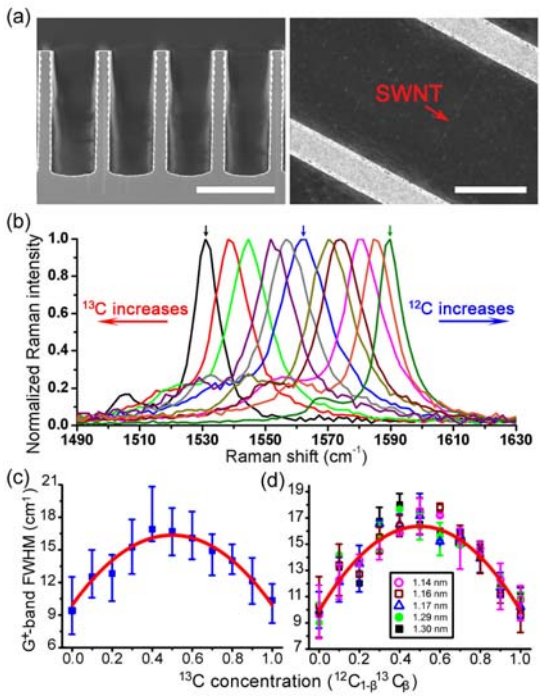

Figure 4. (a) SEM images of a patterned substrate before and after growth of SWNTs. (b) Examples of G^+-band features from 11 ^{13}C concentrations, ranging from $^{12}C_{1.0}{}^{13}C_{0.0}$ (rightmost) $^{12}C_{0.0}{}^{13}C_{1.0}$ (leftmost). (c,d) FWHM value of the Raman G^+-band peaks as a function of the ^{13}C concentration of average SWNTs (c) and SWNTs with specific diameters (d).

SC and DOC have a diameter of approximately 5 nm, and when SDS wraps around SWNTs with different conductivities, the micelles encapsulating metallic SWNT have a larger size (~ 3 nm) compared with those encapsulating semiconducting SWNTs (~ 2 nm). Moreover, DGU results using dual-surfactant DOC and SDS agents demonstrate that the sizes of SWNT-surfactant micelles are enlarged by the addition of SDS, to approximately 7 nm.

5. Isotope-induced elastic scattering of Γ -point optical phonons in SWNTs

I investigated the isotope effects on SWNTs, especially those involving the longitudinal optical (LO) and transverse optical (TO) phonons near the Γ-point in the Brillouin zone (BZ), which give rise to the strongest features in resonance Raman spectra of SWNTs.

Scanning electron microscopy (SEM) images of the patterned substrates before and after growth are shown in Figure 4(a). After growth, SWNTs were found suspending across the trenches. Examples of G-band features of SWNTs with 11 different isotope-doping ratios β, ranging from 0% ^{13}C (rightmost, β=0) to 100% ^{13}C (leftmost, β=1), are shown in Figure 4(b). It can be seen that when the ^{13}C concentration in SWNT increases, the G-band peak shifts to lower wavenumbers.[19,20]

Besides of the peak shifts, a peak broadening Width of the G-band features was characterized as another important effect resulting from isotope substitution in SWNTs. For example, compared to 100% ^{13}C-contained SWNTs [black arrow in Figure 4(b)] and 0% (green arrow), the 50% ^{13}C-mixed SWNT (blue arrow), has a much broader G-band peak feature. We plot the FWHM value of the G^+-band peaks as a function of the ^{13}C concentration for all the SWNTs and for some specific diameters in Figure 4(c,d). Quadratic approximations can be adopted for the fittings of these plots, as shown in red curves. The linewidths, for both average values of all SWNTs and individual nanotubes with specific diameter, follow the same symmetry trend, and SWNTs with the most isotope substitution (half of the atoms are substituted) showed up to an 80% broadening in their linewidths.

In a SWNT formed with concentrations β ^{13}C and (1-β) ^{12}C atoms, the scattering probability arising from the presence of isotopes can be expressed as $\beta(1-\beta)/\tau_I$, where τ_I is a representative phonon lifetime due to the isotopes. Because the

phonon lifetime is inversely proportional to the Raman spectra linewidth, the whole linewidth of the Raman LO mode peak can be expressed as:

$$\Gamma = \Gamma_{12} + \beta(1-\beta)\Gamma_I$$

Where Γ_{12} is the linewidth of pure ^{12}C-SWNTs, and Γ_I is the broadenign due to the isotope impurities. This is the reason for the quadratic relation between linewidth and concentration of ^{13}C atoms in SWNTs. Moreover, because of the Kohn anomaly[21] structure in the phonon density of state in SWNTs, elastic scattering of a near Γ-point optical phonon into the LO branch induced by isotopes is permitted by energy and momentum conservation. This elastic scattering shortens the lifetime of the phonons, thus broadening the linewidth of the G-band peaks of the isotope-enriched SWNTs.

6. Conclusions

In summary, I have investigated the separation of SWNT dispersions, and developed an enhanced DGU separation by introducing SDS into a DOC-dispersed SWNT system. This elucidated the morphology formed by these two surfactants, in which SDS is loading into the space between the ordered DOC on the nanotube surface. Moreover, by increasing the loading of SDS, the separation can be further broadened and enhanced, suggesting a potential of improving the efficacy of the DGU technique.

I have also investigated the Raman spectra from isotope-mixed suspended SWNTs. The results show that the induced mass fluctuation, together with the special Kohn anomaly structure in the SWNT LO phonon branch, results in increased elastic scatterings of optical phonons into this branch. This research can provide further understanding on the phonon decay process in SWNTs.

ACKNOWLEDGEMENTS

I am thankful to my collaborators at Rice University and Toho University for their collaboration on many of these experiments.

REFERENCES

[1] Iijima, S.; Ichihashi, T. *Nature* **1993**, *363*, 603.

[2] Jorio, A.; Dresselhaus, G.; Dresselhaus, M. S. *Carbon Nanotubes: Advanced Topics in the Synthesis, Structure, Properties and Applications (Topics in Applied Physics)* (Springer, 2008).

[3] Arnold, M. S.; Stupp, S. I.; Hersam, M. C. Nano Lett. 2005, 5, 713.

[4] Arnold, M. S.; Green, A. A.; Hulvat, J. F.; Stupp, S. I.; Hersam, M. C. Nat. Nanotechnol. 2006, 1, 60.

[5] Maruyama, S.; Kojima, R.; Miyauchi, Y.; Chiashi, S.; Kohno, M. *Chem. Phys. Lett.* **2002**, *360*, 229-234.

[6] Dresselhaus, M. S.; Dresselhaus, G.; Saito, R.; Jorio, A. *Phys. Rep*. **2005**, *409*, 47.

[7] Krupke, R.; Hennrich, F.; Löhneysen, H. V.; Kappes, M. M. *Science* **2003**, *301*, 344.

[8] Zheng, M.; Jagota, A.; Strano, M. S.; Santos, A. P.; Barone, P.; Chou, S. G.; Diner, B. A.; Dresselhaus, M. S.; Mclean, R. S.; Onoa, G. B.; Samsonidze, Ge. G.; Semke, E. D.; Usrey, M.; Walls, D. J. *Science* **2003**, *302*, 1545.

[9] Tu, X.; Zheng, M. *Nature* **2009**, *460*, 250.

[10] Ju, S.-Y.; Doll, J.; Sharma, I. Papadimitrakopoulos, F. *Nat. Nanotechnol.* **2008**, *3*, 356.

[11] Nish, A.; Hwang, J.-Y.; Doig, J.; Nicolas, R. J. *Nat. Nanotechnol.* **2007**, *2*, 640.

[12] Arnold, M. S.; Suntivich, J.; Stupp, S. I.; Hersam, M. C. *ACS Nano* **2008**, *2*, 2291.

[13] Angelikopoulos, P.; Bock, H. *J. Phys. Chem. B* **2008**, *112*, 13793.

[14] Patel, N.; Egorov, S. A. *J. Am. Chem. Soc.* **2005**, *127*, 14124.

[15] Tummala, N. R.; Striolo, A. *ACS Nano* **2009**, *3*, 595.

[16] Qiao, R.; Ke, P. C. *J. Am. Chem. Soc.* **2006**, *128*, 13656.

[17] Richard, C.; Balavoine, F.; Schultz, P.; Ebbesen, T. W.; Mioskowski, C. *Science* **2003**, *300*, 775.

[18] Yurekli, K.; Mitchell, C. A.; Krishnamoorti, R. *J. Am. Chem. Soc.* **2004**, *126*, 9902.

[19] Liu, L.; Fan, S. S. *J. Am. Chem. Soc*. **2001**, *123*, 11502.

[20] Miyauchi, Y.; Maruyama, S. *Phys. Rev. B* **2006**, *74*, 35415.

[21] Piscanec, S.; Lazzeri, M.; Mauri, F.;. Ferrari, A. C.; Robertson. J. *Phys. Rev. Lett.* **2004,** *93*, 185503.